

# Mechanism of proton transport in water clusters and the effect of electric fields: a DFT study

Nam H. Vu<sup>1,2,3</sup>, Hieu C. Dong<sup>1,2</sup>, My V. Nguyen<sup>1,2</sup>, Thang Bach Phan<sup>1,2,\*</sup>, Dzung Hoang<sup>1,2</sup>, Thuat T. Trinh<sup>4,\*</sup>

<sup>1</sup> Center for Innovative Materials and Architectures (INOMAR), Vietnam National University in Ho Chi Minh City, Vietnam

<sup>2</sup> Vietnam National University, Ho Chi Minh City, Vietnam

<sup>3</sup> Faculty of Materials Science and Technology, University of Science, Vietnam National University in Ho Chi Minh City, Vietnam

<sup>4</sup> Department of Civil and Environmental Engineering, Norwegian University of Science and Technology, S.P Andersen vei 5, 7491-Trondheim, Norway

E-mail: [thuat.trinh@ntnu.no](mailto:thuat.trinh@ntnu.no), [pbthang@inomar.edu.vn](mailto:pbthang@inomar.edu.vn)

**Abstract.** Proton transport inside metal organics frameworks (MOFs) plays an important role to understand and develop a new type of material for a high conductivity application. One of the possible pathways of this process is via water cluster which is confined inside the MOFs structure. In this work, the mechanism of proton transport is investigated within the Density Functional Theory (DFT) calculations. Different water clusters from dimer to pentamer and octamer, which are equivalent to water structures inside the tetrahedral and cubic cavities of MOF-801, respectively, were systematically considered. The results show that proton transfer inside the pentamer cluster has the lowest barrier around 16 kJ/mol. Moreover, the presence of electric fields has a strong effect on the mechanism and energy profile of the proton transfer in both pentamer and octamer cluster. Our DFT prediction of proton migration energies is supported by experimental data of high conducting MOFs such as MOF-801.

*Keywords:* Density Functional Theory, water cluster, proton transport, Electric fields

## 1. Introduction

The development of renewable energy sources such as fuel cell, solar energy, wind, geothermal, biomass has played a significant role in the energy sector in the recent years. Fuel cell is an appealing energy conversion system for generating electricity with renewable energy source from hydrogen, methanol or ethanol. Because of its advantage such as low emission, high power density and fast start-up feature, proton exchange membrane fuel cell is among the most promising approach [1, 2]. Within a standard fuel cell system  $H_2/O_2$ , the proton passes to the cathode through the proton membrane, transforming the chemical energy into electrical energy. Thus, the developing new material with high proton conductivity at high temperature and high relative humidity has become more and more importance in science and technology. Metalorganic frameworks (MOFs) have a great potential for this purpose [3-5]. One recent example was provided by Mukhopadhyay et al. [6] to fabricate nanocomposite membranes with MOFs and polymer by solution casting blending method with enhanced or better properties for fuel cell application. Another work by Paul et al. [7] has shown that a novel MOF/Aquivion composite membrane exhibited enhanced proton conductivity compared with the Nafion. This material could be a promising candidate for designing a robust polymer electrode membrane for electrochemical applications [7]. There are several reviews were recently published on this important topic of proton conduction in MOFs [8-10]. As an example, MOF-801 [11] and VNU-15 [12] were reported to have very high proton conductivity properties. Thus, the understanding of the mechanism of proton transfer inside MOFs is great of importance. There were several works devoted to study the proton transfer in this kind of material. Considering liquid water as the media for proton transfer inside MOFs, activation energy of the process was calculated with empirical potential [13, 14]. The proton transport mechanism in aqueous environment with ab-initio molecular dynamics was

also investigated previously [15-18]. However, the most stable water structure inside MOF-801 was found tetrahedral and cubic cavities are not in the liquid form but rather in the form of pentamer and octamer water cluster [19]. The structural properties of these cluster were reported earlier by using DFT calculations [20-23]. More recently, the hydrogen bonding structure of confined liquid water inside MOF was studied by Reith et al. [24]. However, the possibility for proton transport via water clusters inside the MOF environment are limited. To the best of our knowledge, such mechanism was not reported.

Recently, the impact of electrical field on MOF's structure and properties was reported [25-27]. The possibility of using external electrical fields as a further stimulus to trigger structural changes in MOFs has been investigated. For example, the breathing behavior of MIL-53(Cr) occurs by applying the external electrical field [25]. Transport of gas through metal-organic framework membranes (MOFs) can be strongly influenced by the external electrical field [26]. However, the effect of an external electric field on the transfer of protons inside MOF was little known.

The aims of this paper were to identify all possible key steps in the proton transfer process in the water dimer, pentamer and octamer cluster. Reaction energy and activation energy of the proton transfer between water molecules will be studied. Importantly, we will also consider the effect of electric field on the proton transfer process. The proton transfer in water cluster will be studied in the presence of an electric fields with different strength and orientation.

## **2. Computational Methods**

All DFT calculations were performed in Gaussian 16 package [28]. The B3LYP functional [29] was employed with aug-cc-PVDZ basis set to optimize the geometry and to scan reaction coordinates for the proton transfer process. Our setup with B3LYP functional

was verified to yield a good agreement with the literature for the benchmarking water dimer (see Table S1 in SI). We obtained the binding energy, which is defined as the energy difference between the optimized dimer and two optimized monomers, of 19.7 kJ/mol which is in good agreement with literature value [30-33]. In addition, B3LYP was used extensively in previous studies of proton transfer in water environment [34-36]. Therefore, the choice of this method seems reasonable for the balance between computing cost and accuracy. By taking into account the Zero-Point Energy (ZPE) corrections, this binding energy reduced to 10.9 kJ/mol from our calculations. The later value is also consistent with previous theoretical studies for the water-dimer case [37, 38]. The effect of ZPE correction to the energy profile of proton transfer in the case of water dimer is reported in the SI. The activation barrier for dimer cluster at  $d_{O-O} = 2.8 \text{ \AA}$  reduces by 9 kJ/mol with ZPE corrections. The observation provided the same trend as found in literatures [37, 38]. However, extending the ZPE corrections for binding energies of our system of pentamer and octamer clusters including all geometry point along the energy profile would require expensive computing power. Therefore, the ZPE corrections were not included in our energy values within this paper. More benchmark on the dimer binding energy (with various DFT functional and basis set) and the effect of the CPCM solvation model are presented in Fig. S2 and Table S1 in SI. Our aim was to simulate the water cluster that was not in contact with the liquid water, so in our setup the solvation correction was not taken into account. We have tested the effect of basis set superposition error (BSSE) for the binding energy of dimer, trimer, pentamer and octamer and presented in the Table S2 in SI. Our results are in consistent with previous literatures [37, 39, 40]. The contribution of the BSSE to the total binding energy of water cluster is only around 1 kJ/mol per water-water interaction. We believe that the BSSE has no effect on the activation barrier of the proton transfer inside the water cluster. Therefore, BSSE was not

included explicitly in our further calculations for the energy barrier of proton transfer. We could estimate that the BSSE effect to the activation barrier is around 5%.

While proton transport in water dimer was investigated earlier, we are revisiting the case with extended calculation on the effect of electric field. Since those clusters were found in the MOF, the pentamer and octamer water cluster were also chosen (see Table S3-S5 in SI). In such a large water cluster, the function of the water molecule is not only the interaction with H-bonds, but also the transportation path of protons from one water molecule to another. Dozens of possible conformers of pentamer [20], octamer [21, 41] water cluster and their protonated structures [42, 43] were reported previously in literatures. However, we limited ourself in the conformers of double trimer and cubic octamer that were found in the MOF-801 material with water fully loaded as described in the experimental work [19]. There are two stable conformers with symmetry  $S_4$  and  $D_{2d}$  for the cubic shape of octamer water clusters [44]. To obtain the transition state of a chemical reaction, there are two common methods namely the optimization of TS (either with Berny algorithm or Synchronous Transit-Guided Quasi-Newton STQN in Gaussian package) and the scan reaction coordinate. The later method was used previously in literature for the proton transfer process [45] where the energy barrier depends on the distance of oxygen atoms. Thus, we employed the scan reaction coordinate method in our work. The oxygen-oxygen distance was fixed at the optimum value during the reaction coordinate scan for pentamer and octamer structures. This geometric constraint was aimed to mimic the confinement effect of the MOF-801 material and to avoid the transformation of pentamer and octamer into its more stable structures in vacuum [20, 23]. During the scan, the distance between  $H^+$  and oxygen of  $H_2O$  was selected as reaction coordinate for the proton transfer reaction. This distance was varied from 0.9 Å to 1.8 - 2.0 Å.

For simplicity, the relative reaction coordinate at 0 indicates the reactant state, at 1 indicates the product state. Note that during the scan procedure, the other parameters were relaxed to be able to obtain the most possible smooth energy profile (see Fig. S3 and S5 in SI). The energy of the transition state,  $E_{TS}$ , was considered as the maximum point along the energy profile. We calculated the activation energy of the forward reaction  $E_a^f$ , activation energy of the backward reaction  $E_a^b$ , and reaction energy  $E_r$ , respectively as:

$$E_a^f = E_{TS} - E_{reactant} \quad (1)$$

$$E_a^b = E_{TS} - E_{product} \quad (2)$$

$$E_r = E_{product} - E_{reactant} \quad (3)$$

with  $E_{reactant}$ ,  $E_{product}$  and  $E_{TS}$  are the energies of the reactants and products, and transition state respectively. The effect of strength and direction of electric fields to the reaction barrier was calculated with algorithm implemented within Gaussian 16 package [28].

### 3. Results and discussion

#### 3.1. Water dimer cluster

The activation barrier  $E_a$  of the proton transfer in dimer depends on the distance between two oxygen atoms. In the absence of electric fields,  $E_a$  increases from 5 kJ/mol to 40 kJ/mol when increasing the distance O-O from 2.6 Å to 2.9 Å (see Fig. S1 in SI). This result is in a good agreement with previous studies [45]. The effect of electrical fields to the structural properties of water cluster was previously investigated [46-48]. In this study, with the presence of electrical fields of 0.01 au in the same direction with proton transfer ( $\alpha = 0^\circ$ ), the energy of the product shifted toward higher value and thus the later increases in a comparison with those of the reactant. We find that the activation energy  $E_a$  increases with the presence

of electric fields. The rise in activation energy depends on the strength and orientation of electric fields. For example, in the case of  $d_{O-O} = 2.78 \text{ \AA}$ , the activation barrier decreases with the rise of angle between electric fields and proton transfer direction (see in Fig 1.c). The results shows that only at  $\alpha = 90^\circ$ , the energy profiles of proton transfer have a symmetric shape. In other angles, the energy of product goes higher than the reactant. The less angle is the more energy raise. This indicates a significant effect of electrical field to the proton transfer process. The direction and the strength of the electric fields play an important role to the energy barrier. Fig 1.d shows that barrier of forward and backward transfers could alter 100% when varying the strength of electric fields from 0.0001 to 0.01 au. The more the electric field increases, the more activation energy barrier of the forward reaction rises. The opposite trends were observed for the backward reaction.

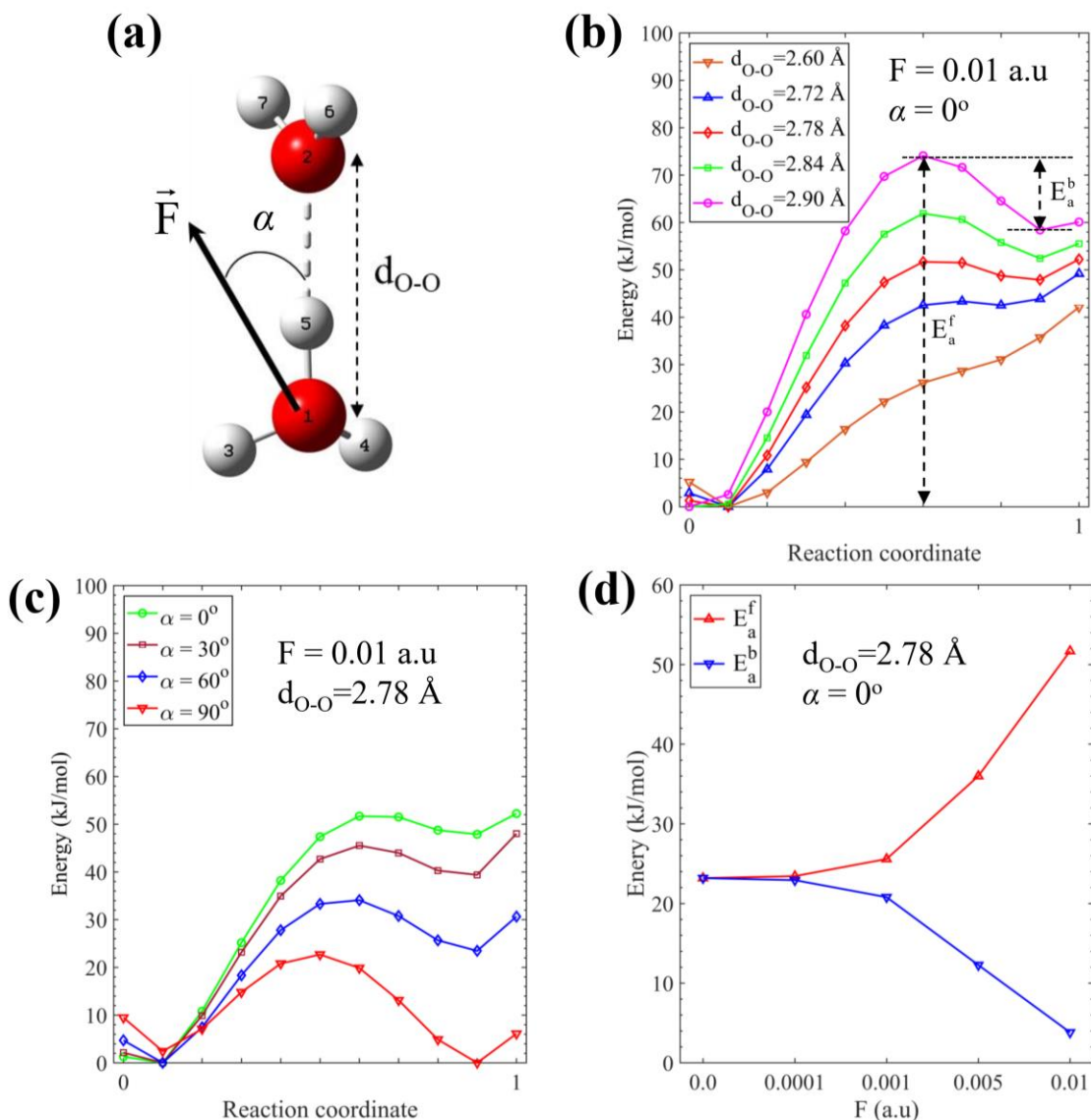


**Figure 1.** The proton transfer process in water dimer cluster at oxygen-oxygen distance  $d_{O-O}$  in the presence of an electric field  $F$  placed at an angle  $\alpha$  (a). The energy profiles along the reaction coordinates of the proton transfer process in dimer in an electric field of 0.01 au with various values of  $d_{O-O}$  (b), with various angle  $\alpha$  (c) The activation energy of proton transfer in dimer at different strength of electric fields (d). More discussions are presented in the text.

### 3.2. Water trimer cluster

The transfer of protons to the water trimer cluster also plays a key role in the entire transfer process. Compared to the dimer cluster, we measured the proton energy transfer profile of the trimer cluster as shown in Fig 2. The distance between oxygen atoms and the angle between the water molecule is an important geometric parameter that has a strong



impact on the activation barrier and the proton transfer reaction barrier. For example, the optimal  $angle_{O-O-O}$  of the water trimer is  $120^\circ$  as shown in Fig. 2.a. Keeping that angle, we scanned the reaction coordinate of the proton transfer reaction at  $d_{O-O}$  equal to  $2.8 \text{ \AA}$  and  $2.9 \text{ \AA}$ . The energy profile shows that the activation barrier for both forward and backward reactions is higher with a longer oxygen-oxygen length. This is consistent with the dimer case when the activation energy increases with an increase in the distance between two water molecules. The reaction energy of the proton transfer reaction in trimer is  $-37 \text{ kJ/mol}$ , which clearly indicates that the proton  $H^+$  prefers to be located in the second water molecule. Taking the  $d_{O-O} = 2.8 \text{ \AA}$ , we studied the effect of the angle between water molecule  $angle_{O-O-O}$  in the range of  $80^\circ - 140^\circ$ . It is noteworthy that the reaction barrier and the reaction energy are only slightly dependent on  $angle_{O-O-O}$  (Fig 2.c). The activation energy of the forward direction, the backward direction, is roughly  $10 \text{ kJ/mol}$  and  $40 \text{ kJ/mol}$  respectively. Fig. 2.d presented the effect of the electric field on the transfer of the proton in trimer. We used the strength of the  $F = 0.01 \text{ au}$  and the  $\alpha = 90^\circ$  as an example. In accordance with the case of dimer, the presence of an electrical field decreases the activation barrier of the forward reaction while increasing the activation barrier of the backward direction. As a result, the reaction energy is around  $20 \text{ kJ/mol}$  more stable than in the case without the presence of electric field. Again, the  $angle_{O-O-O}$  in the range of  $80^\circ - 140^\circ$  shows a minor effect on the activation energy and reaction energy (Fig 2.d).

### 3.3. Pentamer and octamer water cluster

We have learned that the activation energy of proton transfer in dimer will be proportional with the strength of the electric field. Therefore, to reduce the complexity in the case of pentamer and octamer water, only orientation of electric field was investigated. For

these cases, the strength of electric field was selected as 0.01 au, which is similar to other works [49, 50].

We remind that we only considered the conformer structures of pentamer and octamer water clusters which were found in tetrahedral and octahedral cavities of MOF-801 crystal at very high humidity [19]. Hence, to investigate the mechanism of proton transfer inside these clusters is of importance. To simulate this process, we selected the oxygen atom  $O_1$  with an excess  $H^+$ . After that, this  $H^+$  will transfer from one water to another one via proton transfer  $T_{ij}$  from oxygen  $O_i$  to  $O_j$ . Note that in the whole process, the distance O-O was fixed at the initial value at 2.78 Å. We assumed that the adsorbed water cluster in MOFs is confined, therefore, has less flexibility to change its structure during proton transfer process.

We have analysed all possibility of the individual transfer process with more details provided in Table S6-S16 in SI. In the absence of electric fields, the most favourable pathway for proton transport is via oxygen  $O_1$ - $O_5$ - $O_3$ - $O_2$ . Note that in this transfer path, a lower energy was found when  $H^+$  was at  $O_5$  (see Fig 3.b). However, this position the proton was trapped and has no possibility to escape out of the cluster, therefore further proton transfer lead to  $O_2$  is more favourable. The overall activation barrier was calculated as 15.7 kJ/mol. This value is lower than the case of water dimer (20 kJ/mol). However, the activation barrier of the proton transport in our pentamer cluster is higher than that reported by Moon et al.[51] on ice surface ( $10 \pm 3$  kJ/mol). With presence of electric fields in the direction of  $O_1O_4$  and  $O_1O_5$ , the most favourable pathway are  $O_1$ - $O_5$ - $O_3$ - $O_2$  and  $O_1$ - $O_5$ - $O_4$ , respectively. This is because the angle between electric fields and the first proton transfer step was different in the two cases. As the results, the barriers were reported as 16.6 kJ/mol and 49.4 kJ/mol for the direction  $O_1O_4$  and  $O_1O_5$ , respectively. We also observed at the increasing of activation barriers follow by the decreasing of the reaction energy in the case of  $F_{O_1O_4}$ . However, there is a significant

unfavorable of both reaction energy and activation barrier with the presence of electric fields in direction  $O_1O_5$  (see Table 1).

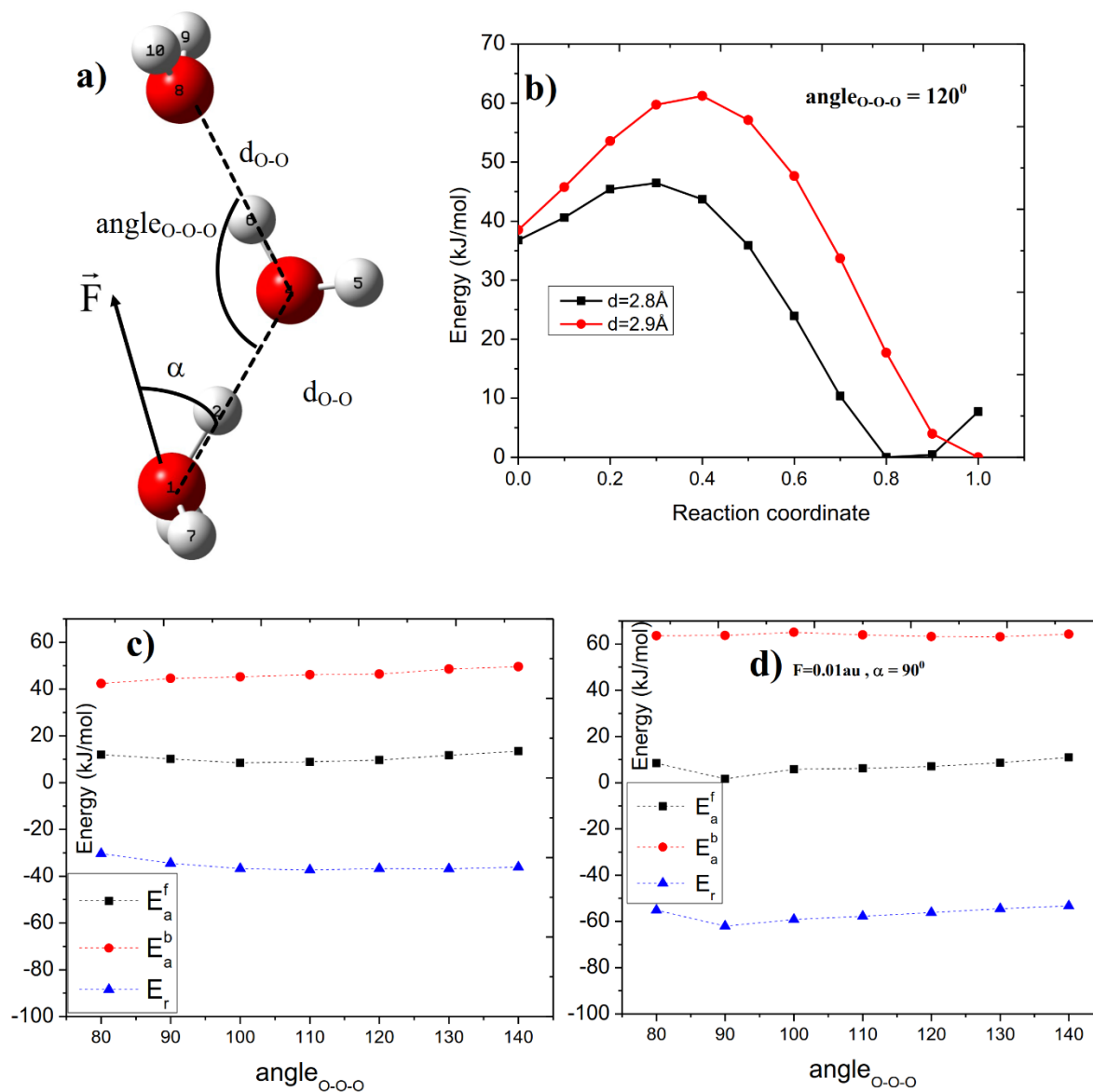


**Figure 2.** The proton transfer process in water trimer cluster (a). The energy profiles of the proton transfer process along the reaction coordinates in trimer cluster at various  $d_{O-O}$  and the optimum angle (b). The effect of  $angle_{O-O-O}$  to the activation and reaction energies in the case without electric field (c) and with electric field of 0.01 au (d). More discussions are presented in the text.

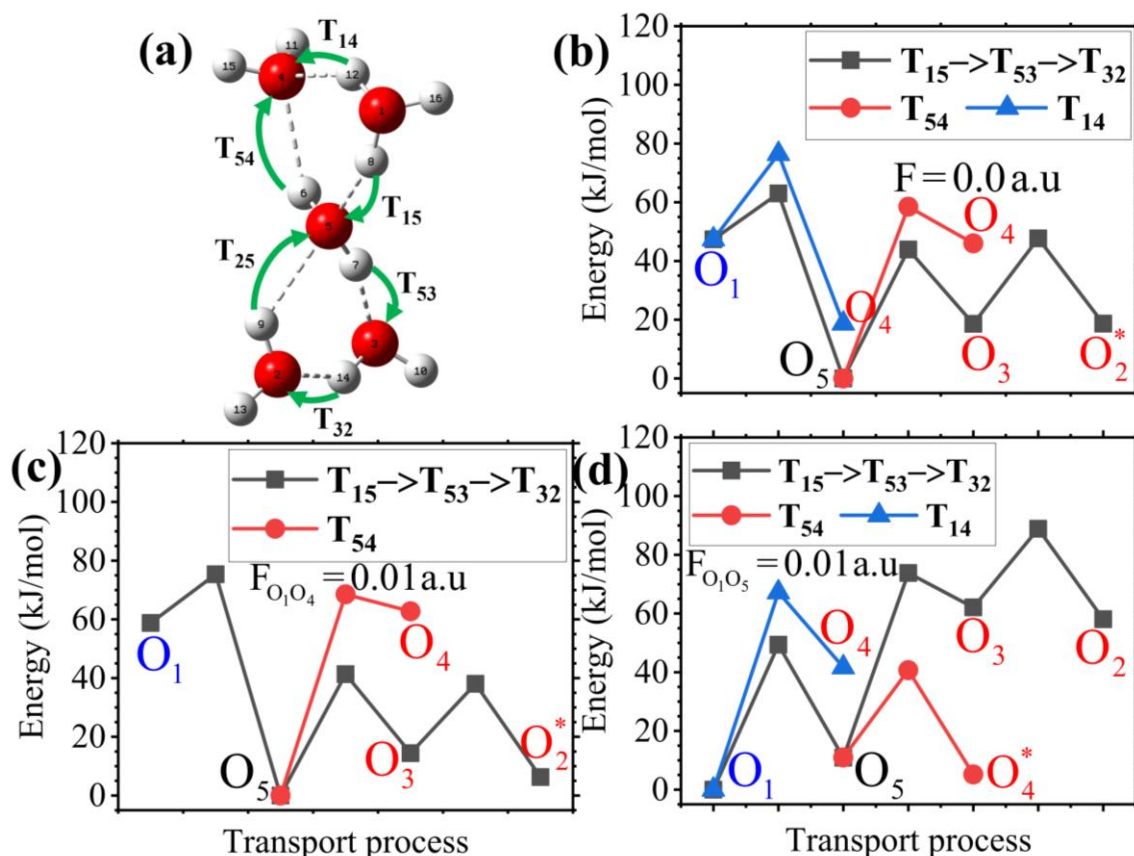


**Figure 3.** The proton transfer process in confined pentamer water cluster with the initial excess proton in oxygen  $O_1$  and the transfer  $T_{ij}$  indicates the direction of proton transfer from oxygen  $i$  to oxygen  $j$ . (a). Various proton transport process from oxygen  $O_1$  to other oxygen in the case of no electric fields (b), in the case of electric fields in direction  $O_1O_4$  (c) and  $O_1O_5$  (d). The blue, black and red color of oxygen atoms indicate the initial proton, no-proton-out and proton-out oxygen, respectively. The oxygen  $O^*$  is the last step of the most favourable proton transport process.

The most favourable of proton transport in water octamer cluster with symmetry  $S_4$  and  $D_{2d}$  are depicted in Fig. 4 and Fig. 5, respectively. It is very interesting to note that the most feasible proton transport of these two clusters is different even in the case without electric fields. The most favourable pathway for  $S_4$  is  $O_1$ - $O_4$ - $O_8$ , while for  $D_{2d}$  is  $O_1$ - $O_2$ . The activation barrier for  $D_{2d}$  is slightly lower than that of  $S_4$  (17.3 kJ/mol and 20.6 kJ/mol). However, the reaction energy  $\Delta E$  of the proton transfer process in  $D_{2d}$  is 26 kJ/mol higher than that in  $S_4$  (-63.4 kJ/mol and -89.0 kJ/mol). In the presence of electric fields at different directions ( $O_1O_2$ ,  $O_1O_7$ , and  $O_1O_5$ ), the activation barrier of the whole proton transport process always increases.

The most unfavourable direction raise almost triple the value of activation barrier when compared with the case without electric fields (see Table 1 for more values). Moreover, the gain in reaction energy was not significant in the most of cases with the presence of electric fields. Compared to the pentamer cluster, the proton transport pathway is longer for octamer cluster. In electric fields, the most feasible pathways contain almost all oxygen atoms in the cluster, hence the distance to transfer proton from oxygen  $O_1$  to the final exist proton was significant longer than that without electric fields.

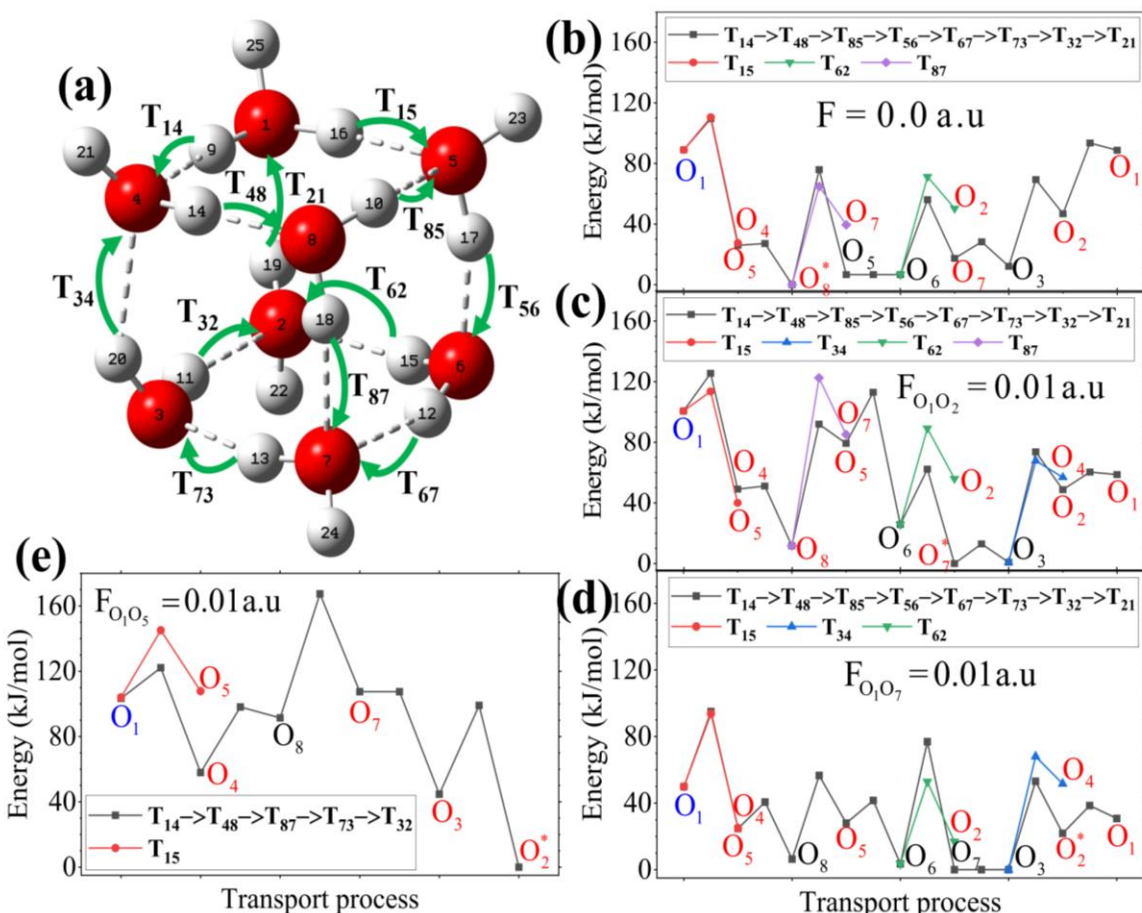


**Figure 4.** The proton transfer process in octamer  $S_4$  water cluster with the initial excess proton in oxygen  $O_1$  (a). Various proton transport process from oxygen  $O_1$  to other oxygen in the case of no electric fields (b), in the case of electric fields in direction  $O_1O_2$  (c),  $O_1O_7$  (d) and  $O_1O_5$  (e). The blue, black and red color of oxygen atoms indicate the initial proton, no-proton-out and proton-out oxygen, respectively. The oxygen  $O^*$  is the last step of the most favourable proton transport process.

### 3.4. The effect of electric fields

It is already known that external electric fields have a strong effect on the equilibrium geometry of water cluster {42-4 ?????}. This work unravels the role of electric fields on the proton transfer mechanism of various water cluster. For the simplest case of water dimer, the results show both positive and negative effects on the activation energy of proton transfer. Not only the angle between the fields and transfer direction but also the the strength of the fields play an important role. The more the strength of the fields is, the more increasing of the activation barrier in the forward direction and reducing in the backward direction (Fig. 1.d)

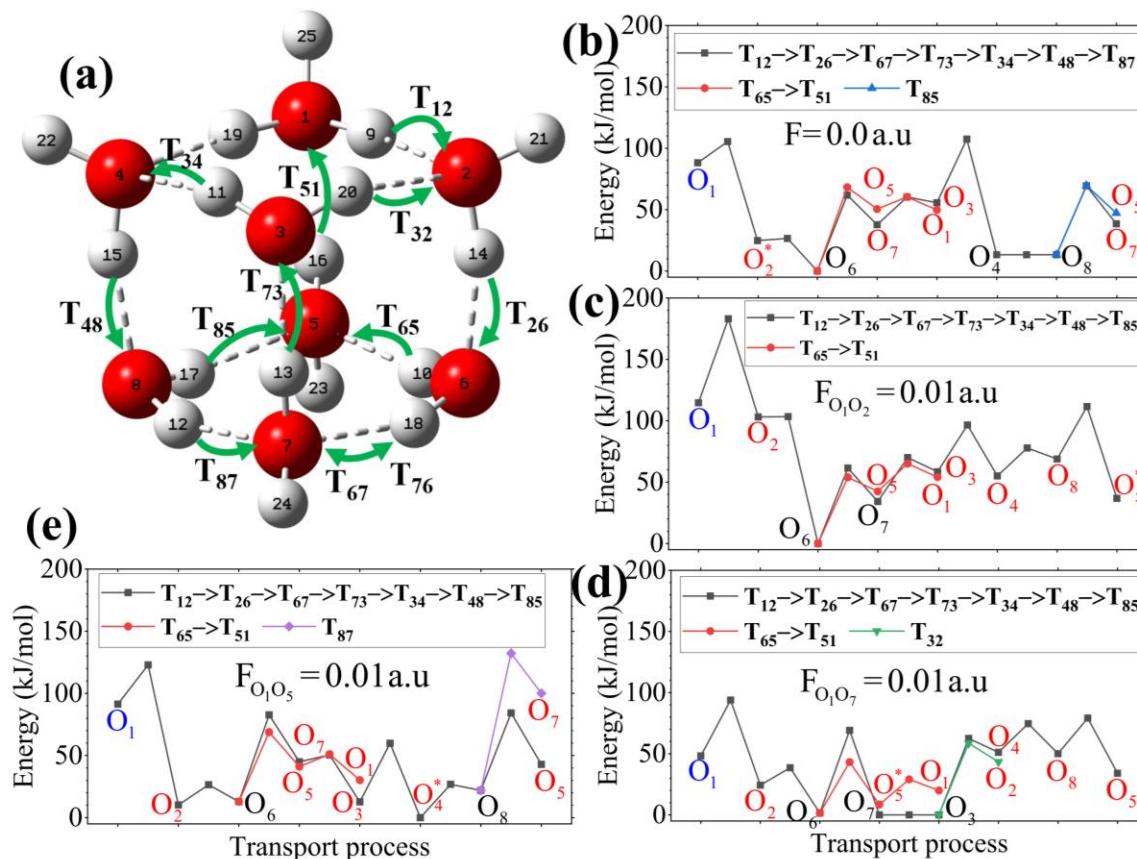


**Figure 5.** The proton transfer process in octamer  $D_{2d}$  water cluster with the initial excess proton in oxygen  $O_1$  (a). Various proton transport process from oxygen  $O_1$  to other oxygen in the case of no electric fields (b), in the case of electric fields in direction  $O_2O_2$  (c),  $O_1O_7$  (d) and  $O_1O_5$  (e). The blue, black and red color of oxygen atoms indicate the initial proton, no-proton-out and proton-out oxygen, respectively. The oxygen  $O^*$  is the last step of the most favourable proton transport process.

The effects of electric fields are not any more simple in the case of more complex water cluster such as pentamer and octamer cluster. Since there are many possible pathways for proton transfer from one water molecule to another molecule in those clusters, the angle between the external fields and proton transfer direction cannot keep the same as the first step. Therefore, it is very difficult to find an optimal angle to reduce the activation energy of the whole proton transfer process. The results show that for pentamer and octamer, the activation energy of proton transfer in the presence of electric fields always higher than that without electric fields. Depends on the initial angle, the increasing of the activation energy might up to three times (Table 1). Moreover, the presence of the electric fields also greatly increases the shortest proton transfer path. For example, the proton only needs to be transferred via two oxygen atoms for the octamer  $D_{2d}$ . As electric field is positioned in the direction  $O_1O_2$ , it must go through all eight oxygen atoms. This work demonstrated a negative effect of an electric field on the proton transfer reaction in complex water clusters. Thus, to design materials with high proton conductivity, the undesirable effects of external electric fields should be avoided.

**Table 1.** Reaction energy  $\Delta E$  (kJ/mol) and activation energy  $E_a$  (kJ/mol) of the most favorable proton transfer process in various confined water clusters and the effect of electric fields of 0.01 au. The angle between the electric fields and the first proton transfer step  $\alpha$  ( $^\circ$ ) are presented.

Water structure	Electric fields	Transport process	$\Delta E$	$E_a$	$\alpha$
Pentamer	$F = 0$	$O_1-O_5-O_3-O_2$	-28.8	15.7	
	$F_{O_1O_4}$	$O_1-O_5-O_3-O_2$	-52.5	16.6	60
	$F_{O_1O_5}$	$O_1-O_5-O_4$	5.2	49.4	0
Octamer $S_4$	$F = 0$	$O_1-O_4-O_8$	-89.0	20.6	
	$F_{O_1O_2}$	$O_1-O_4-O_8-O_5-O_6-O_7$	-100.6	24.9	90
	$F_{O_1O_7}$	$O_1-O_4-O_8-O_5-O_6-O_2$	-33.0	45.1	55
	$F_{O_1O_5}$	$O_1-O_4-O_8-O_7-O_3-O_2$	-103.4	64.1	90
Octamer $D_{2d}$	$F = 0$	$O_1-O_2$	-63.4	17.3	
	$F_{O_1O_2}$	$O_1-O_2-O_6-O_7-O_3-O_4-O_8-O_5$	-77.9	68.4	0
	$F_{O_1O_7}$	$O_1-O_2-O_6-O_5$	-39.7	45.7	57
	$F_{O_1O_5}$	$O_1-O_2-O_6-O_7-O_3-O_4$	-91.3	31.6	92

#### 4. Conclusions

In conclusion, this work presented first-principles investigation on the proton transfer process in the water cluster from dimer to octamer structures. In the case of the dimer and trimer cluster, a fundamental insight was given. The proton transfer activation barrier is strongly controlled by the distance between water molecules. Though there are small effects on the activation barriers of the angles between the water molecules. The power and direction of the electric field has a strong effect to enlarge the energy difference between the forward and the backward reactions.

For larger water cluster, the total reaction energy for proton transfer of  $D_{2d}$  and  $S_4$  octamer water clusters is more favourable than that of pentamer. We obtained the value of activation energy around 16-20 kJ/mol for these types of cluster, which are in good agreement with experimental data for proton transfer in MOFs material. It is important to observe that the activation barrier and reaction energy depends on size and the symmetry the water cluster. The results are more pronounced in the presence of an electric field. It is found that electric fields located in different directions have significant effects on the pathways, thermodynamics and kinetics of proton transfer. These effects lead mostly to an increase in proton migration energy and, at the same time, to a decrease in reaction energy. It is important to note that the MOF cluster will be in a disorganized orientation in a real application. It is, therefore, very difficult to control the direction of the electrical field in the entire MOF. However, as stated in our study, there is a negative effect on the pathway and barrier of proton transfer in the presence of an electrical field. Therefore, it is desirable to avoid the influence of electric fields in order to design MOFs, ZIFs material with high proton-conductivity application.

A limitation of this work is that the interaction between confined water cluster and MOF framework was not taken into account due to an expensive computational cost for such a full



system. The interaction with the MOF with the water cluster contributes mainly to the stabilization of the water cluster. In this study, our focus was on the transfer of protons internally within the water cluster, so we expected the impact of the MOF structure to be relatively small here. However, we are aware that this MOF-water interaction may be important for the transfer of water outside the water cluster, such as proton from MOF to water via the hydrogen bonding network. This study is served as a first and fundamental step toward investigation of the possibility for proton transfer mechanism through water clusters. This is a complimentary to the idea of proton transfer via liquid water inside MOFs, ZIPs materials. Further investigation using a less expensive method such as QM/MM or semiempirical and the dynamics of the proton transport of water cluster in an explicit MOF environment is highly desirable to give a more details picture of the process.

### **Acknowledgments**

This work was supported by Vietnam National University in Ho Chi Minh city under grant B2018-50-01. Computational resources were supported by the National Center for High-Performing Computing (NCHC) and the 238-Cluster at Institute of Atomic and Molecular Science, Academia Sinica in Taiwan. The authors would like to thank Dr. Jer-Lai Kuo and Prof. Duc Nguyen-Manh for fruitful discussion and to thank anonymous reviewers for valuable comments and suggestions.

### **Conflict of interest**

The authors declare that they have no conflict of interest.

## Supporting Information

See supplementary material for more DFT benchmark results, geometries of water cluster in xyz format and the energy profile along proton transport inside water clusters.

## References

- [1] B.C.H. Steele, A. Heinzl, *Nature*, 414 (2001) 345-352.
- [2] D. Larcher, J.M. Tarascon, *Nature Chemistry*, 7 (2015) 19-29.
- [3] P. Ramaswamy, N.E. Wong, G.K.H. Shimizu, *Chemical Society Reviews*, 43 (2014) 5913-5932.
- [4] A.-L. Li, Q. Gao, J. Xu, X.-H. Bu, *Coordination Chemistry Reviews*, 344 (2017) 54-82.
- [5] G.K.H. Shimizu, J.M. Taylor, S. Kim, *Science*, 341 (2013) 354.
- [6] S. Mukhopadhyay, A. Das, T. Jana, S.K. Das, *ACS Applied Energy Materials*, 3 (2020) 7964-7977.
- [7] S. Paul, S.-J. Choi, H.J. Kim, *Energy & Fuels*, 34 (2020) 10067-10077.
- [8] X.-X. Xie, Y.-C. Yang, B.-H. Dou, Z.-F. Li, G. Li, *Coordination Chemistry Reviews*, 403 (2020) 213100.
- [9] Y. Ye, L. Gong, S. Xiang, Z. Zhang, B. Chen, *Advanced Materials*, 32 (2020) 1907090.
- [10] W.-H. Li, W.-H. Deng, G.-E. Wang, G. Xu, *EnergyChem*, 2 (2020) 100029.
- [11] J. Zhang, H.-J. Bai, Q. Ren, H.-B. Luo, X.-M. Ren, Z.-F. Tian, S. Lu, *ACS Applied Materials & Interfaces*, 10 (2018) 28656-28663.
- [12] T.N. Tu, N.Q. Phan, T.T. Vu, H.L. Nguyen, K.E. Cordova, H. Furukawa, *Journal of Materials Chemistry A*, 4 (2016) 3638-3641.
- [13] F. Paesani, *The Journal of Physical Chemistry C*, 117 (2013) 19508-19516.
- [14] D.D. Borges, S. Devautour-Vinot, H. Jobic, J. Ollivier, F. Nouar, R. Semino, T. Devic, C. Serre, F. Paesani, G. Maurin, *Angewandte Chemie International Edition*, 55 (2016) 3919-3924.
- [15] B.F. Habenicht, S.J. Paddison, M.E. Tuckerman, *Physical Chemistry Chemical Physics*, 12 (2010) 8728-8732.
- [16] G.A. Ludueña, T.D. Kühne, D. Sebastiani, *Chemistry of Materials*, 23 (2011) 1424-1429.
- [17] M. Tuckerman, K. Laasonen, M. Sprik, M. Parrinello, *The Journal of Chemical Physics*, 103 (1995) 150-161.
- [18] J.A. Morrone, K.E. Haslinger, M.E. Tuckerman, *The Journal of Physical Chemistry B*, 110 (2006) 3712-3720.
- [19] H. Furukawa, F. Gándara, Y.-B. Zhang, J. Jiang, W.L. Queen, M.R. Hudson, O.M. Yaghi, *Journal of the American Chemical Society*, 136 (2014) 4369-4381.
- [20] F. Ramírez, C.Z. Hadad, D. Guerra, J. David, A. Restrepo, *Chemical Physics Letters*, 507 (2011) 229-233.
- [21] J. Kim, B.J. Mhin, S.J. Lee, K.S. Kim, *Chemical Physics Letters*, 219 (1994) 243-246.
- [22] A. Ünal, U. Bozkaya, *International Journal of Quantum Chemistry*, 120 (2020) e26100.
- [23] P. Qian, W. Song, L. Lu, Z. Yang, *International Journal of Quantum Chemistry*, 110 (2010) 1923-1937.

- [24] A.J. Rieth, K.M. Hunter, M. Dincă, F. Paesani, *Nature Communications*, 10 (2019) 4771.
- [25] A. Ghoufi, K. Benhamed, L. Boukli-Hacene, G. Maurin, *ACS Central Science*, 3 (2017) 394-398.
- [26] A. Knebel, B. Geppert, K. Volgmann, D.I. Kolokolov, A.G. Stepanov, J. Twiefel, P. Heitjans, D. Volkmer, J. Caro, *Science*, 358 (2017) 347.
- [27] J.P. Dürholt, B.F. Jahromi, R. Schmid, *ACS Central Science*, 5 (2019) 1440-1448.
- [28] M.J. Frisch, G.W. Trucks, H.B. Schlegel, G.E. Scuseria, M.A. Robb, J.R. Cheeseman, G. Scalmani, V. Barone, G.A. Petersson, H. Nakatsuji, X. Li, M. Caricato, A.V. Marenich, J. Bloino, B.G. Janesko, R. Gomperts, B. Mennucci, H.P. Hratchian, J.V. Ortiz, A.F. Izmaylov, J.L. Sonnenberg, Williams, F. Ding, F. Lipparini, F. Egidi, J. Goings, B. Peng, A. Petrone, T. Henderson, D. Ranasinghe, V.G. Zakrzewski, J. Gao, N. Rega, G. Zheng, W. Liang, M. Hada, M. Ehara, K. Toyota, R. Fukuda, J. Hasegawa, M. Ishida, T. Nakajima, Y. Honda, O. Kitao, H. Nakai, T. Vreven, K. Throssell, J.A. Montgomery Jr., J.E. Peralta, F. Ogliaro, M.J. Bearpark, J.J. Heyd, E.N. Brothers, K.N. Kudin, V.N. Staroverov, T.A. Keith, R. Kobayashi, J. Normand, K. Raghavachari, A.P. Rendell, J.C. Burant, S.S. Iyengar, J. Tomasi, M. Cossi, J.M. Millam, M. Klene, C. Adamo, R. Cammi, J.W. Ochterski, R.L. Martin, K. Morokuma, O. Farkas, J.B. Foresman, D.J. Fox, Wallingford, CT, 2016.
- [29] A.D. Becke, *Physical Review A*, 38 (1988) 3098-3100.
- [30] J.R. Lane, *Journal of chemical theory and computation*, 9 (2013) 316-323.
- [31] X. Xu, W.A. Goddard, *The Journal of Physical Chemistry A*, 108 (2004) 2305-2313.
- [32] V.S. Bryantsev, M.S. Diallo, A.C.T. van Duin, W.A. Goddard, *Journal of chemical theory and computation*, 5 (2009) 1016-1026.
- [33] C. Leforestier, K. Szalewicz, A. van der Avoird, *The Journal of Chemical Physics*, 137 (2012) 014305.
- [34] C. Lao-ngam, P. Asawakun, S. Wannarat, K. Sagarik, *Physical Chemistry Chemical Physics*, 13 (2011) 4562-4575.
- [35] A.A. Tulub, *The Journal of Chemical Physics*, 120 (2004) 1217-1222.
- [36] G. Meraj, M. Naganathappa, A. Chaudhari, *International Journal of Quantum Chemistry*, 112 (2012) 1439-1448.
- [37] A. Mukhopadhyay, S.S. Xantheas, R.J. Saykally, *Chemical Physics Letters*, 700 (2018) 163-175.
- [38] R.E.A. Kelly, J. Tennyson, G.C. Groenenboom, A. van der Avoird, *Journal of Quantitative Spectroscopy and Radiative Transfer*, 111 (2010) 1262-1276.
- [39] C.K. Kim, J. Won, C.K. Kim, *Chemical Physics Letters*, 545 (2012) 112-117.
- [40] L. Zhang, H. Zhang, Y.M. Kwon, N. Shahzad, H. Chen, X. Wang, A. Liu, L. Zhang, D. Zhu, X. Xia, D. Gao, C.K. Kim, *Industrial & Engineering Chemistry Research*, 59 (2020) 13290-13304.
- [41] P. Nigra, M.A. Carignano, S. Kais, *The Journal of Chemical Physics*, 115 (2001) 2621-2628.
- [42] J.-L. Kuo, M.L. Klein, *The Journal of Chemical Physics*, 122 (2004) 024516.
- [43] Q.C. Nguyen, Y.S. Ong, J.L. Kuo, *Journal of chemical theory and computation*, 5 (2009) 2629-2639.
- [44] S.S. Xantheas, E. Aprà, *The Journal of Chemical Physics*, 120 (2003) 823-828.
- [45] S. Kondati Natarajan, T. Morawietz, J. Behler, *Physical Chemistry Chemical Physics*, 17 (2015) 8356-8371.
- [46] Y.C. Choi, C. Pak, K.S. Kim, *The Journal of Chemical Physics*, 124 (2006) 094308.
- [47] D. Rai, A.D. Kulkarni, S.P. Gejji, R.K. Pathak, *The Journal of Chemical Physics*, 128 (2008) 034310.

- [48] D. Rai, A.D. Kulkarni, S.P. Gejji, L.J. Bartolotti, R.K. Pathak, *The Journal of Chemical Physics*, 138 (2013) 044304.
- [49] A. Huzayyin, J.H. Chang, K. Lian, F. Dawson, *The Journal of Physical Chemistry C*, 118 (2014) 3459-3470.
- [50] P. Marracino, M. Liberti, G. d'Inzeo, F. Apollonio, *Bioelectromagnetics*, 36 (2015) 377-385.
- [51] E.-S. Moon, J. Yoon, H. Kang, *The Journal of Chemical Physics*, 133 (2010) 044709.